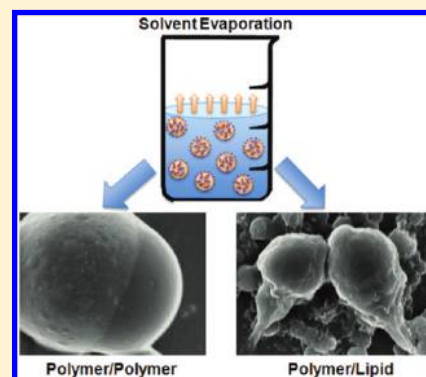


# Production and Characterization of Anisotropic Particles from Biodegradable Materials

Francis S. Romanski, Jennifer S. Winkler, Ryan C. Riccobene, and M. Silvana Tomassone\*

Chemical and Biochemical Engineering, Rutgers University, 98 Brett Road, Piscataway, New Jersey 08854, United States

**ABSTRACT:** In recent years, production and characterization of anisotropic particles has become of interest in a wide range of scientific fields including polymer chemistry, drug delivery, electronics, energy, and nanotechnology. In this work, we demonstrate a novel formulation for production of anisotropic particles via an internal phase separation of biodegradable components. Specifically, binary mixtures of biodegradable polymers poly(lactic-co-glycolic acid), polycaprolactone, and biodegradable lipid Precirol (glyceryl palmitostearate) were dissolved in dichloromethane, emulsified, and prepared into anisotropic particles using a modified solvent evaporation technique. During the slow evaporation process the components self-assembled into anisotropic particles with distinct morphologies. Polymer/polymer formulations resulted in compartmentalized anisotropic heterodimer particles, while polymer/lipid combinations yielded “ice cream cone” shaped particles. It was found that addition of certain active pharmaceuticals resulted in an altered, pox-like segregation at the particle surface of polymer/polymer formulations. The anisotropic nature of the particles was subsequently characterized using optical microscopy, scanning electron microscopy, zeta potential, electrophoresis, and X-ray diffraction. Successful formulations presented here may potentially be employed as multi-compartmental drug carriers with staggered drug release rates or alternatively as a colloidal excipient for an arsenal of pharmaceutical applications.



## 1. INTRODUCTION

In recent years, anisotropic particles containing two distinct surfaces with differential chemical or physical properties have been a major focus of scientific research due to their unique amphiphilic surface, potential for self-assembly, and limitless applications.<sup>1–3</sup> While the pursuit of anisotropic particles has been widespread and thorough, there is one area of research where anisotropic particles are just beginning to find their niche: the pharmaceutical industry. Here, biodegradable anisotropic particles could potentially offer compartmentalization of reactive agents, dual-release profiles of active components, or simultaneous loading of vastly dissimilar compounds within a single particle. The ability to incorporate drugs and other active components into multiphasic systems with long-term stability has remained a key aim for the pharmaceutical industry. Therefore, this industry would greatly benefit from the use of anisotropic particles in place of any potentially cytotoxic or environmentally hazardous compounds currently used or, alternatively, for establishing new anisotropic particle-based formulations.

Currently, the materials used in the current synthesis of anisotropic particles are not generally recognized as safe (GRAS) by the FDA and as such are excluded from use in drug carriers or other products intended for human consumption. For example, many anisotropic particles are currently created using poly(methyl methacrylate) (PMMA), polystyrene, or even clays like laponite, all of which are not easily introduced into the body.<sup>3–5</sup> Although many different polymeric anisotropic particles have been synthesized, current

methods typically rely on microfluidic devices that are capable of producing just one single particle at a time with an average yield on the order of tens of grams per day.<sup>6</sup> In addition, there are also limitations regarding the fluid compatibility with microfluidic devices; only fluids with low viscosity, negligible viscoelastic response, and moderate interfacial tension meet the criteria for drop formation. These constraints severely restrict or exclude the use of lipid-based biodegradable materials commonly used in pharmaceutical products.<sup>7</sup> Thus, there is a critical need to develop an innovative approach for synthesis of biocompatible, biodegradable Janus particles for drug delivery, tissue engineering, self-assembly of biomaterials, and countless other biological applications.<sup>8</sup>

In this work, we demonstrate a novel formulation and modified solvent evaporation method capable of producing large quantities of anisotropic biodegradable micro- and nanoparticles (ABMPs and ABNPs). The output achieved by this one-pot synthesis approach is limited only by physical parameters such as the amount of starting material and capacity of processing equipment. The biodegradable excipients used as building blocks for anisotropic particle formation in this work are not only GRAS substances but also frequently used in the pharmaceutical industry for drug encapsulation.<sup>9–11</sup> The remainder of this article is as follows: section 2 describes in detail the methods used to produce anisotropic biodegradable

**Received:** November 14, 2011

**Revised:** January 19, 2012

**Published:** January 27, 2012

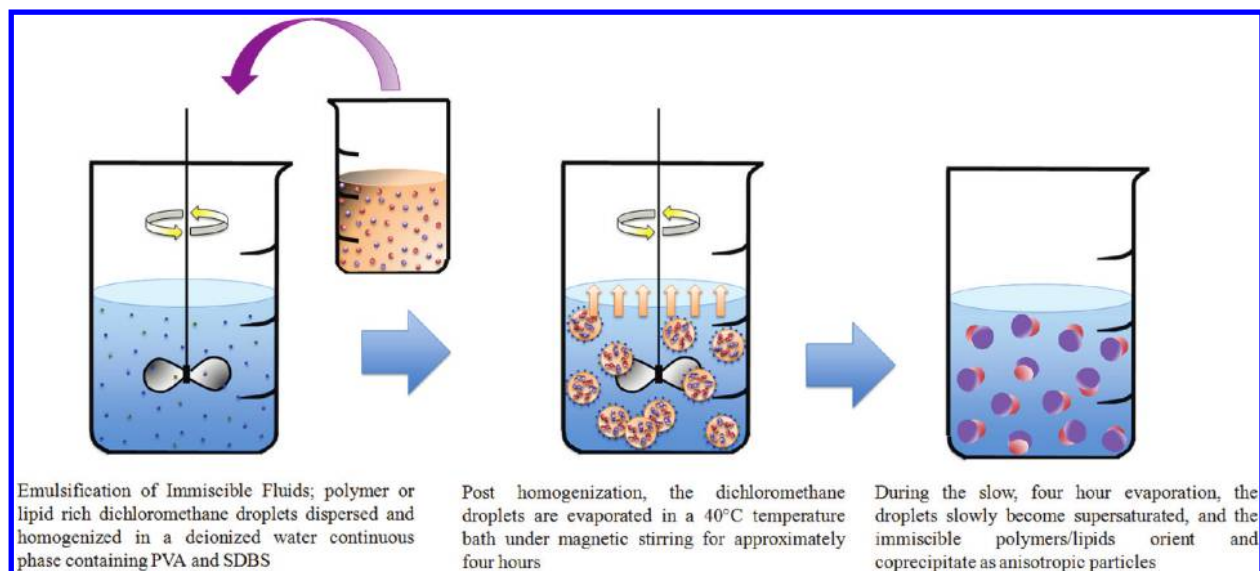


**Figure 1.** Schematic representation of the experimental methodology for production of biodegradable anisotropic particles.

particles. Section 3 describes the results obtained and several novel characterization methods used to describe the anisotropic behavior and a thorough discussion of potential applications. Finally, section 4 describes the conclusions reached in this work and ideas for future directions.

## 2. MATERIALS AND METHODS

**2.1. Summary of the Materials.** Standard O/W emulsions were produced using dichloromethane (DCM) as the dispersed phase solvent; it was purchased from Sigma Aldrich (USA) and used as received. The continuous phase was deionized water produced from the Millipore system. Poly(lactic-co-glycolic acid) (PLGA) (MW 40 000–75 000; 65:35 lactic acid:glycolic acid; P2066) and polycaprolactone (PCL) (MW 42 500–65 000; 181609) were each purchased from Sigma Aldrich (USA) and used as received. Precirol ATO 5 glycerol distearate type I EP was obtained from Gattefossé SAS (Saint-Priest Cedex, France) and used as received. Surfactants polyvinyl alcohol (PVA), sodium dodecyl sulfate (SDS), and sodium dodecyl benzylsulfate (SDBS) were each purchased from Sigma Aldrich and used as received.

**2.2. Methodology.** ABMPs and ABNPs were produced by dissolving a 50:50 mass ratio of PLGA (0.50 g) and PCL (0.50 g) into a 40 g solution of DCM using a magnetic stirrer. The water phase was created with 100 g of deionized water containing 0.30 g of PVA and 0.10 g of SDBS. After all components were dissolved the two phases were mixed and emulsified using the Ultra Turrax T-25 rotor-stator at 5000 rpm for 5 min. The emulsion was transferred to a Chemglass double-walled beaker (Chemglass, Inc. Vineland, NJ). The open beaker was kept at a constant temperature of 40 °C and magnetically stirred at a constant 125 rpm for 4 h. A schematic of the experimental procedure is shown in Figure 1.

Polymer/lipid ABMPs (“ice cream cone particles”) were produced by dissolving a 75:25 mass ratio of either PLGA (0.75 g) or PCL (0.75 g) with Precirol ATO 5 (0.25 g) into a 40 g solution of DCM using a magnetic stirrer. The water phase contained 100 g of deionized water, 0.30 g of PVA, and 0.10 g of SDBS. After dissolution, the mixture was emulsified using the Ultra Turrax T-25 rotor-stator at 5000 rpm for 5 min. The emulsion was transferred to a Chemglass double-walled beaker. The open beaker was kept at a constant temperature of 40 °C and magnetically stirred at a constant 125 rpm for 4 h.

Larger particles were synthesized for use with optical microscopy using identical steps to those above except for the emulsification step. The two-phase mixture system was emulsified by manually shaking for 5 min instead of a rotor-stator. Applying less shear resulted in significantly larger emulsion droplets and ultimately larger particles.

The larger droplets required longer evaporation times, approximately 6 h on average. Ultrafine nanoscale particles, or ABNPs, were produced by first using the Ultra Turrax T-25 for 5 min at 5000 rpm and subsequently using the Emulsiflex C-3 high-pressure homogenizer (Avestin, Inc., Ottawa, Canada) for three high-pressure cycles at 500 bar.

**2.3. Summary of Analytical Equipment Used.** Size analysis was performed using a Beckman-Coulter LS-13 320 Laser Diffraction apparatus. Samples were run for combined obscuration and polarization intensity differential scattering (PIDS) analysis. A refractive index of 1.476 was used to define the particles. Zeta-potential measurements were conducted using the Beckman-Coulter DelsaNano C low-concentration cell. Optical microscope images and videos were taken using a Celestron 44350 LCD Digital LDM Biological Microscope. Electrophoresis images were produced by applying an electric potential of 1.5 V across a sample of suspended particles on the microscope slide. X-ray diffraction was carried out using a Phillips X’Pert Powder X-ray Diffraction unit. Samples were tested from 10° to 90° at a sensitivity of 0.01. Scanning electron microscope (SEM) images were acquired using the Amray 1830 I scanning electron microscope. Samples were prepared by centrifuging suspensions for 30 min at 5000 rpm. The supernatant was removed, and particles were spread on top of the silicon wafer with a laboratory spoon. Samples were vacuum desiccated and sputter coated with carbon using a Balzers SCD 004 Sputter Coating Unit prior to imaging.

## 3. RESULTS AND DISCUSSION

Section 3.1 describes the synthesis and size distributions of ABMPs. Section 3.2 describes polymer/lipid ABMPs termed “ice cream cone” particles. Next, section 3.3 describes the observed and hypothesized formation kinetics. Section 3.4 describes the loading of particles with various types of drug and the observed changes in the phase segregation behavior. Section 3.5 describes several different indirect characterization methods for analyzing the anisotropic behavior of the particles. Finally, section 3.6 describes the nearly limitless possibilities of ABMPs.

**3.1. Synthesis of Polymer/Polymer Anisotropic Particles.** Anisotropic biodegradable microparticles and nanoparticles (ABMPs and ABNPs) were produced using a 4-h solvent evaporation process. The size of the particles was determined using laser diffraction. To explore the attainable size region, particles containing 50:50 PLGA:PCL mixtures

were produced using three different levels of shear including high-pressure homogenization (high energy), rotor-stator homogenization (moderate energy), and manual shaking (low energy); the resulting particle size distributions postevaporation are shown in Figure 2. It should be noted that the use of high-

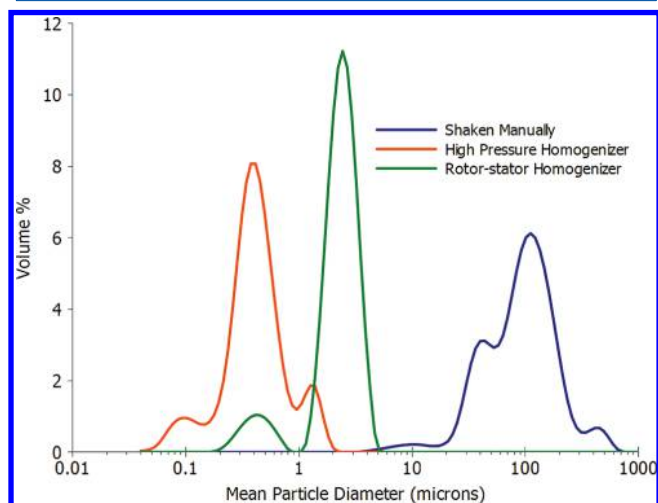


**Figure 2.** Laser diffraction produced particle size distributions for hybrid PLGA and PCL (50:50) particles produced high-pressure homogenization for ultrafine particles (ABNPs), rotor-stator homogenizer for micrometer scale particles (ABMPs), and manually shaken for large particles.

pressure homogenization yielded ABNPs small enough to be classified as submicrometer or even nanoscale from a pharmaceutical industry perspective.<sup>12</sup>

Unfortunately, ABNPs produced with a rotor-stator in combination with high-pressure homogenization were far too small to systematically evaluate anisotropic behavior. Therefore, only larger particles produced by manual shaking were used for

visual characterization using optical and scanning electron microscopy. Figure 3 displays a series of SEM images of 50:50 PLGA:PCL particles produced using manual shear. The images suggest a bifurcation of the two polymers at an interface. In addition, a textural difference between the two polymers was observed; the larger of the two phases exhibited a surface roughening. After imaging each polymer individually it was determined that PCL had a much rougher surface than PLGA, and therefore, the PCL is the larger of the two phases. It was found that the PLGA and PCL retained their individual surface characteristics in the PLGA:PCL particles. Densities of 1.22 and 1.14 g/cm<sup>3</sup> have been established for virgin PCL and PLGA, respectively, which further indicates that the larger of the two phases is indeed PCL.<sup>13</sup>

In order to further define the apparent anisotropy displayed by the ABMPs, 50 mg of Sudan Red III was introduced into the system. Sudan Red III is a common food additive used to dye oils and hydrophobic components in the food and pharmaceutical industries. Initially, the particles exhibited a pinkish hue and no selective coloring of either particle compartment. However, after 24 h the dye diffused to the more hydrophobic PCL compartment of the particles. An optical microscope image of the dyed ABMPs clearly exhibiting anisotropy is shown in Figure 4.

### 3.2. Synthesis of Polymer/Lipid Anisotropic Particles.

The polymer/polymer particles exhibited anisotropy despite the fact that PLGA and PCL are very similar in material property. This observation led to the realization that using formulations containing materials of dissimilar material properties can increase the anisotropic character of the particles. Lipids were chosen to complement the polymeric phase because they are commonly used materials for production of solid lipid nanoparticles (SLNs).<sup>11</sup> Polymer/lipid hybrid particles were synthesized with several goals in mind, including demonstrating the robustness of the process and increasing the degree of anisotropy. Polymer/lipid particles were produced

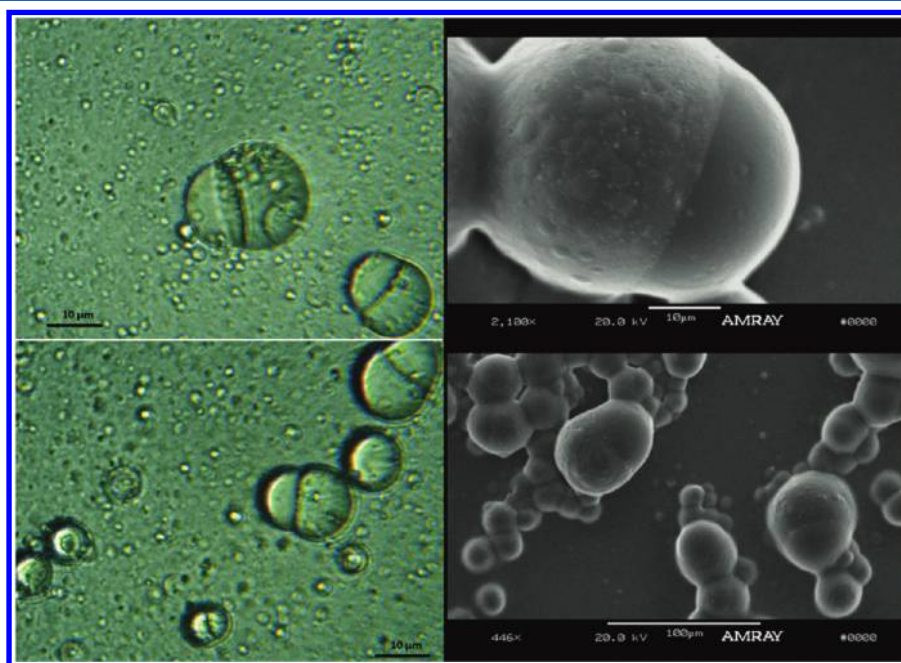


**Figure 3.** Optical microscopy and scanning electron microscopy images for manually produced large anisotropic polymer particles containing 50:50 PLGA to PCL.

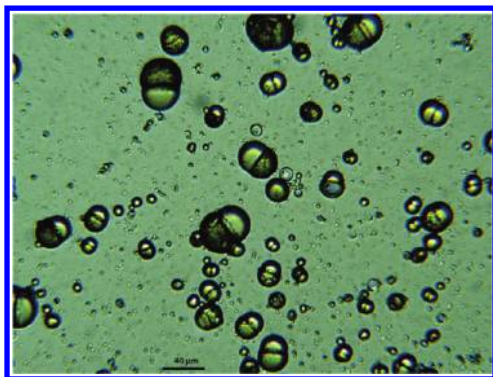


**Figure 4.** Optical microscopy images of dual-polymer particles produced with Sudan Red III and rested for 24 h where the dye evidently migrated to the more hydrophobic PCL side of the particles.

using the same methods as the biphasic polymer particles. After initially testing several ratios it was found that only lipid/polymer ratios of 25:75 or lower resulted in viable particles. At higher lipid concentrations, particles experienced lipid agglomeration and particles of a more amorphous character. Precirol ATO 5 glycerol distearate was used as the hydrophobic phase, and either PLGA or PCL was used as the hydrophilic component with no difference in resulting morphology. Scanning electron and optical microscope images are shown in Figure 5.

The polymer/lipid particles displayed a much more interesting and unexpected morphology than the hemispherical polymer/polymer particles. Specifically, these polymer/lipid particles exhibited a longer, cone-shaped tail bound to a spherical polymer head. The particles were coined “ice cream cone” particles, where the PCL or PLGA head was the hydrophilic “ice cream” head and Precirol was the hydrophobic “cone” tail. The formation mechanism for this unique morphology is discussed in subsequent sections.

### 3.3. Formation Kinetics of the Anisotropic Particles.

Production of larger particles allowed for real-time monitoring of growth kinetics under an optical microscope. Sample aliquots were removed from the double-walled glass chamber and observed at different time intervals throughout the evaporation process. After approximately 3 h of evaporation, dichloromethane droplets nearly reached the saturation level of the constituent polymers. The final stage of particle formation was examined and recorded using the optical microscope. Results are shown in Figure 6.

Through optical microscopy it was revealed that the particles do not nucleate and grow from the side of the droplet as originally hypothesized, but rather, polymer segregation and solidification occur more or less homogeneously during dichloromethane evaporation. After some time, a clear bifurcation line was apparent at the centerline of the particles. The nascent interface slowly became more conspicuous as evaporation proceeded until a clear phase separation appeared at the interface between PLGA and PCL. The presence of an interface provided evidence of increased hydrogen bonding between the two polymers when in forced contact. It was hypothesized that while in the liquid solution phase of the dichloromethane droplet the polymers may be homogeneously dispersed. During the slow evaporation process, the slightly immiscible polymers migrated toward a more entropically favorable state. This drove PLGA and PCL to segregate to opposite poles. During and after precipitation, the two phases were joined together by an interpenetrating polymer network at the equatorial interface. Disordered end chains of the amorphous PLGA lock into more ordered end chains of the crystalline PCL at the interface, and ultimately, the polymers were locked together by hydrogen bonding at the interface. Simply because each droplet is an isolated microreactor the polymers were forced to coprecipitate. Therefore, particle solidification was driven by solvent diffusion and evaporation, provided evaporation remained slow enough to enable the polymer chains to migrate to opposite poles rather than form a

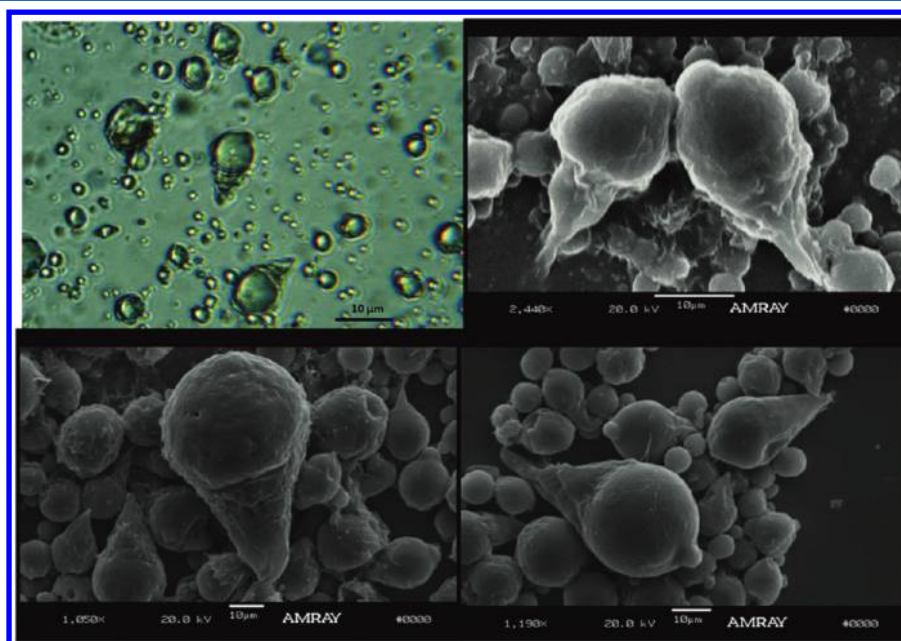


**Figure 5.** Optical microscopy and scanning electron microscope images of particles produced with a 25:75 weight ratio of Precirol (lipid) and PLGA (polymer).

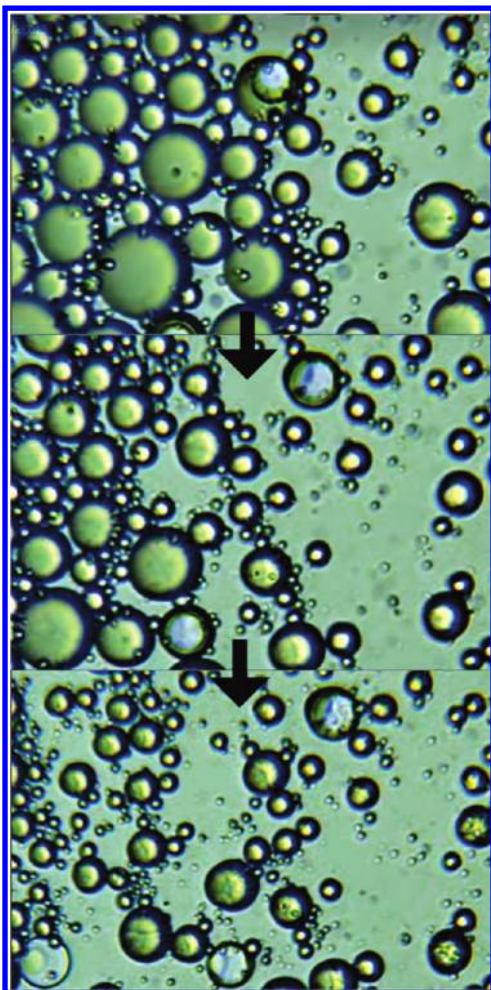


**Figure 6.** Series of optical microscope images illustrating formation of the PCL:PLGA particles.

homogeneous blend. The overall process is represented as a schematic in Figure 7.

Phase segregation of Precirol and PLGA or PCL into “ice cream cone” particles was also observed using optical microscopy. The formation behavior of these particles was entirely different in nature than that of the polymer/polymer particles. Rather than a slow particle segregation analogous to cell division, the lipid Precirol “cone” precipitated long before

the polymer component. Supersaturation of the lipid was reached much faster than that of the polymer, despite the lipid being present at significantly lower levels (25 wt % compared to 75 wt % of polymer). The lipid tail remained at the interface of the droplet as the spherical polymer component was formed. A temporal image of tail precipitation is shown in Figure 8, and

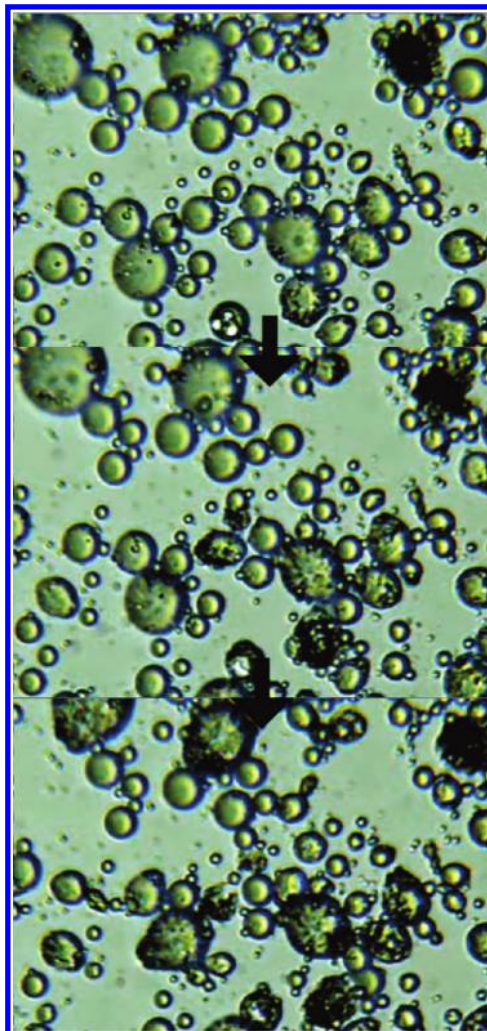


**Figure 8.** Series of optical microscope images illustrating formation of the 25:75 Precirol:PLGA.

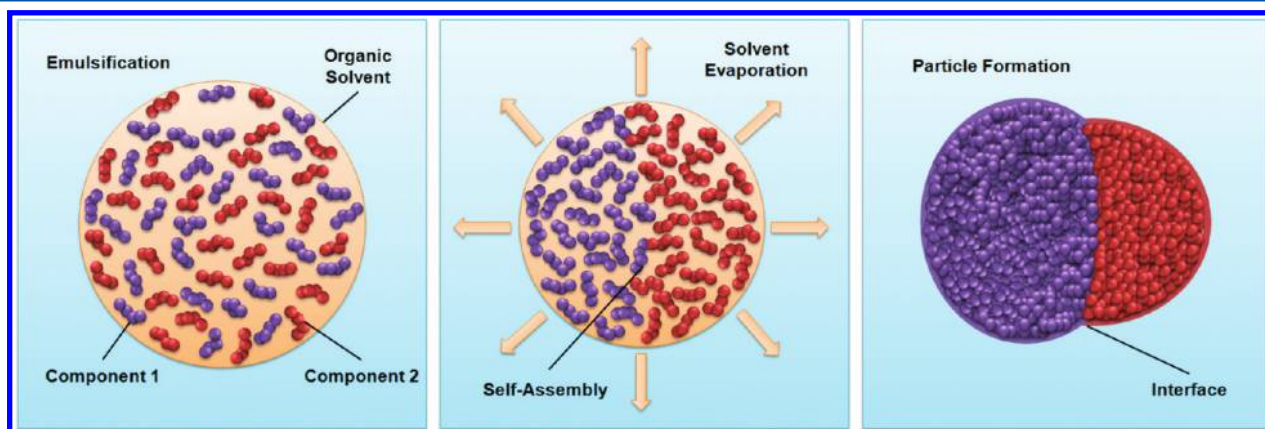


**Figure 7.** Schematic representation of polymer/polymer particle formation.

the corresponding schematic of polymer/lipid particle formation is presented in Figure 9. Through experimentation with

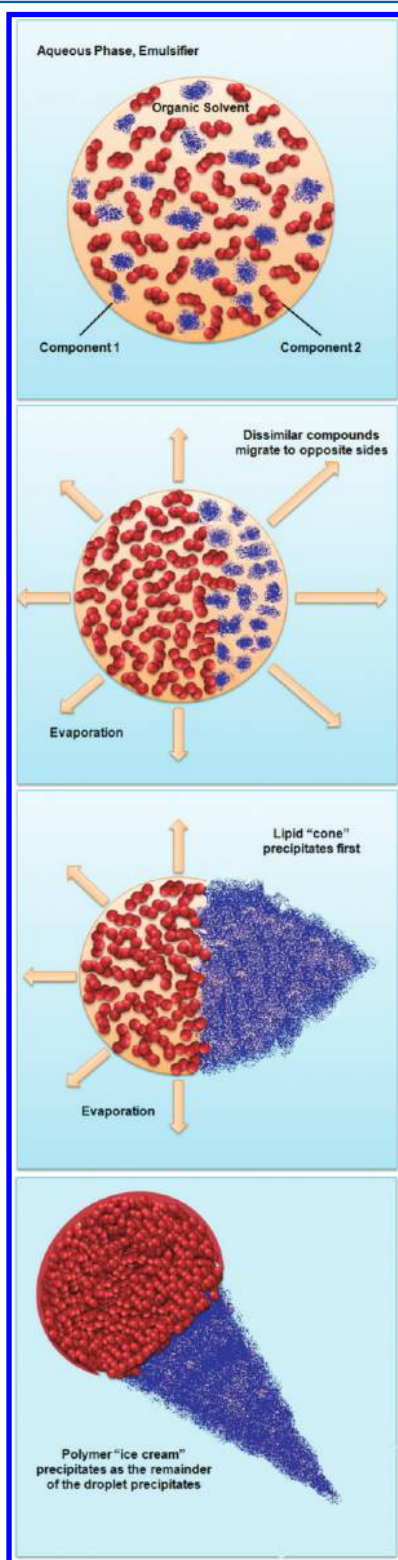


**Figure 9.** Schematic representation of polymer/lipid particle formation.

different formulations it was discovered that the final shape and length of the lipid tail is governed at least in part by interfacial tension. For example, long, slender tails were produced when an identical mass fraction of SDS was used in place of PVA

(SDBS was still used); scanning electron microscope images of these tails are shown in Figure 10. This phenomenon and the importance of additives on formation will be the subject of future investigations.

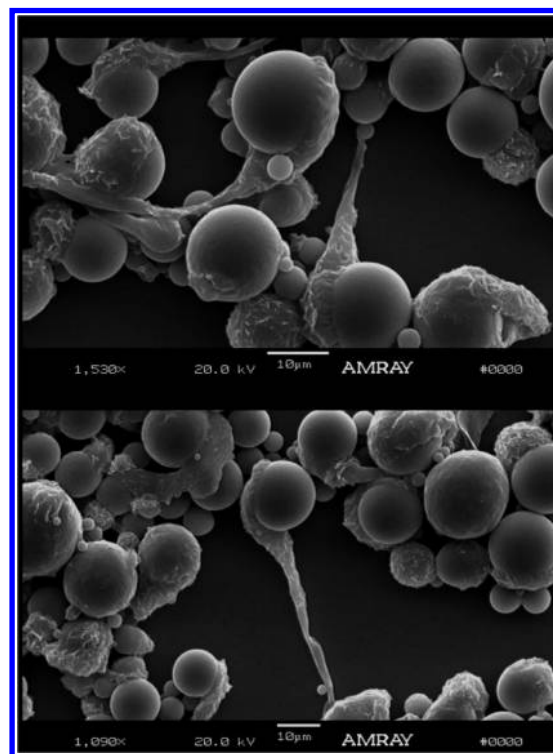


**Figure 10.** Scanning electron microscope images of “ice cream cone” particles produced using SDS as a surfactant (instead of PVA).

**3.4. Drug Loading and the Effect on Phase Segregation.** ABMPs were loaded with drug by codissolving the active agent with the polymer/polymer or polymer/lipid components in the dispersed phase. Although drug loading did not significantly affect formation of polymer/lipid anisotropic particles, it tremendously affected the phase separation of the polymer/polymer particles. Strange, “pox-like particles” were produced when 5% w/w drug was codissolved with PLGA and PCL; this is shown in Figure 11. Three drug systems tested were griseofulvin (poorly water soluble), omeprazole (poorly water soluble), and acetaminophen (water soluble). Each of the three drugs, regardless of intrinsic chemical properties or hydrophobicity ( $\log P = 2.71, 1.66, \text{ and } 0.51$ , respectively) resulted in identical phase separation behavior.<sup>14</sup> Here, small blisters of PLGA segregated onto the surface of the PCL matrix, resulting in pox-like particles rather than compartmentalized anisotropic particles. It is hypothesized that the drug may act as a “compatibilizer”, which reduces the interfacial free energy between the two polymers. Similar structures have been reported for nonbiodegradable polymer/polymer particles by addition of a block-copolymer-containing segments of the two immiscible polymer species.<sup>15</sup>

Figure 11 depicts the effect of adding 5% w/w griseofulvin to a 50:50 mixture of PLGA and PCL on particle morphology. Small crystals of griseofulvin are visible protruding through the polymeric matrix. Griseofulvin is a poorly water-soluble drug with limited polymorphic activity commonly used as a case study for bioavailability enhancement. In order to prevent pox-like particles, the encapsulated material(s) should have limited

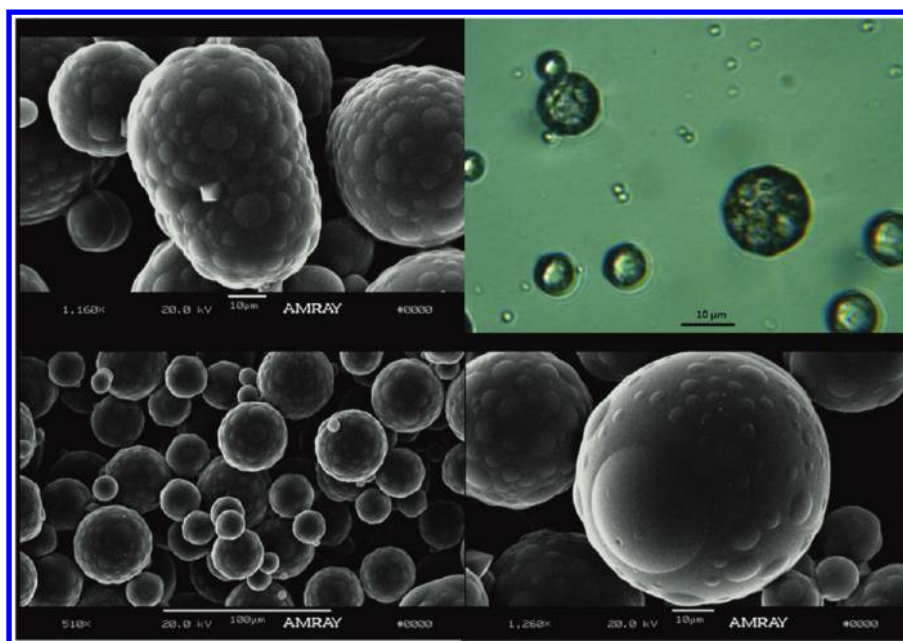


**Figure 11.** Optical microscopy and scanning electron microscope images of particles with a 50:50 weight ratio of PLGA and PCL and containing griseofulvin (5% w/w with polymer).

affinity for the encapsulating polymers. Alternatively, the drugs may be precipitated prior to formation of the anisotropic particles.

**3.5. Characterization of Anisotropic Particles.** ABMPs were further characterized through zeta-potential measurements, electrophoresis, and powder X-ray diffraction. These methods were not applied to ABNPs (nanoscale particles) because of the limitations inherent in visualizing and characterizing nanoparticles. For instance, ABNPs could not be viewed using optical microscopy, were too small to visualize during electrophoresis under the optical microscope, and are too small for accurate X-ray diffraction results. Due to these limitations, the characterization described here is applicable only to ABMPs, with only an assumption that the properties scale down to the nanoregime; this will be tested in future iterations of this work. In many of the examples below particles were produced using only PCL, PLGA, or Precirol alone for comparative purposes; the procedure used to produce the particles was identical to that of the ABMPs.

The zeta potential of the particles was determined using photon correlation spectroscopy. Results are shown in Table 1.

**Table 1. Resulting Zeta Potential of the Anisotropic Particles Produced from Polymer–Polymer, Polymer–Lipid, and Drug-Loaded Formulations**

formulation	zeta potential (mV)
PLGA-alone	$-15.20 \pm 0.35$
PCL-alone	$-17.25 \pm 1.92$
Precirol-alone	$-35.03 \pm 0.31$
PLGA:PCL	$-12.84 \pm 0.77$
PLGA:PCL + 5 wt % Gris.	$-23.20 \pm 0.90$
PLGA:Precirol	$-15.22 \pm 1.78$
PCL:Precirol	$-39.74 \pm 2.58$

Resulting zeta potentials of the polymer/polymer particles, drug-loaded polymer/polymer particles, and polymer/lipid particles were compared against those of the individual

components of the mixtures. Each set of particles was tested in triplicate and averaged. The results are reported as the mean  $\pm$  the standard deviation of the mean. ABMPs produced from an equal mixture of PLGA and PCL had a zeta potential of  $-12.84 \pm 0.77$  mV, slightly lower in absolute value than the  $-15.20 \pm 0.35$  and  $-17.25 \pm 1.92$  mV potentials of PLGA and PCL individually, respectively. It is hypothesized that combining the polymers has an effect on the electrostatic stability of the particles. The zeta potential of Precirol particles alone was  $-35.03 \pm 0.31$  mV. Precirol/PLGA particles had a lower absolute value zeta potential at  $-15.22 \pm 0.78$  mV, while Precirol/PCL particles exhibited a significantly higher absolute value zeta potential at  $-39.74 \pm 2.58$  mV. These findings suggest an electrical anisotropy of both the polymer/polymer and the polymer/lipid particles, which is discussed in detail below. The zeta potential of drug-loaded particles was considerably higher at  $-23.20 \pm 0.90$  mV, indicating incorporation of the drug significantly increases the electrostatic stability of the particles due to the intrinsic charge on the griseofulvin crystals at neutral pH. This result is promising for incorporation of drugs and other compounds into the anisotropic particles.

An electrical field was applied to a sample of larger particles on an uncovered glass slide within the optical microscope to determine electrical anisotropy. A 1.5 V potential was applied across the suspended particles on the microscope slide. The polymer/polymers ABMPs rapidly oriented with the more hydrophobic component, PCL, migrating toward the positively charged anode. Particles relaxed upon removal of the electrical field. The results were recorded as video, and two frames comparing particle orientation in the absence and presence of electrical field are shown in Figure 12. The particles were dyed with Sudan Red III so that the more hydrophobic component could be clearly distinguished. Similar electrophoresis results were observed for the polymer/lipid particles, where the more hydrophobic component Precirol oriented toward the positive anode.

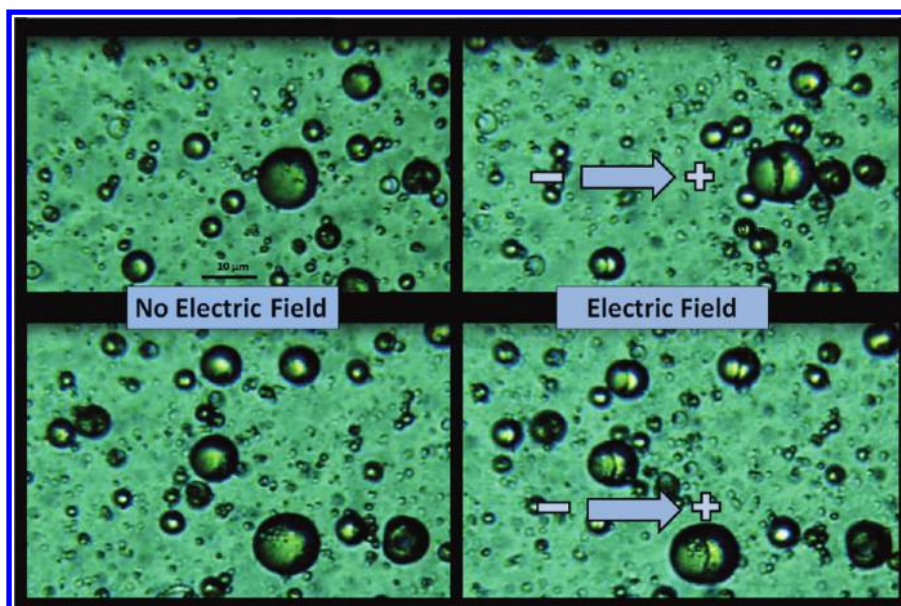


**Figure 12.** Optical microscope images of 50:50 PCL:PLGA particles shown stationary and under an electric field, where the PCL, hydrophobic side always flows toward the positive cathode.

Next, powder X-ray diffraction was performed on PLGA/PCL, drug-loaded PLGA/PCL, PLGA/Precirol, PCL/Precirol, pure PCL, pure PLGA, and griseofulvin micrometer-scale particles. Particles were harvested by centrifugation, dried, and ground to a fine powder prior to testing. In order to increase the likelihood of capturing any signal from X-ray diffraction for the amorphous PLGA and semicrystalline PCL, micrometer-scale ABMPs were tested. All samples exhibited approximately identical mean particle diameters with a single, large diffraction peak in the 1–5  $\mu\text{m}$  range (see Figure 2). Figure 13 displays

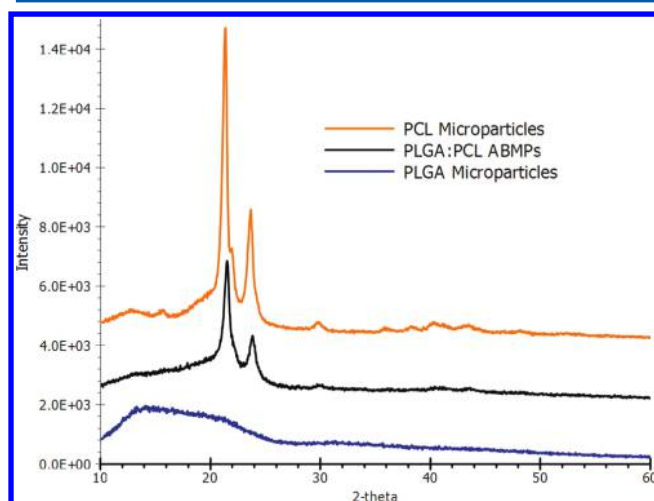


**Figure 13.** X-ray diffraction patterns of (a) PLGA microparticles, (b) PLGA:PCL ABMPs, and (c) PCL microparticles.

patterns of microparticles produced using only PLGA, only PCL, and ABMPs created with a 50:50 mixture of the two. The PLGA diffraction pattern (bottom) indicates an amorphous structure, while the PCL pattern (top) exhibits a clear crystallinity. The diffraction pattern of the 50:50 PLGA/PCL ABMPs (center) is a summation of the diffraction peaks of PLGA and PCL rather than an average. This indicates an

isolated phase of crystalline PCL, confirming compartmentalization and anisotropy.

Griseofulvin-loaded 50:50 PLGA/PCL ABMPs were also analyzed using powder X-ray diffraction and compared against crystalline griseofulvin and the empty PLGA/PCL particles. Diffraction patterns for these microparticles are shown in Figure 14. The pattern for griseofulvin (bottom) reveals high

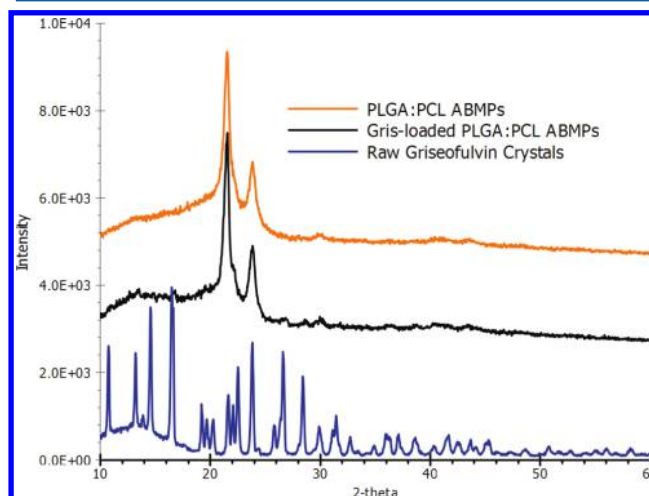


**Figure 14.** X-ray diffraction patterns of (a) griseofulvin, (b) griseofulvin-loaded ABMPs, and (c) PLGA:PCL ABMPs.

crystallinity and is consistent with the literature.<sup>16</sup> The diffraction pattern of the griseofulvin-loaded PLGA/PCL particles (center) retains the overall crystallinity of PCL and resembles that of empty PLGA/PCL particles (top) despite the PLGA surface blisters. This further corroborates the assertion that the presence of drug induces phase segregation without affecting the structure of either polymer. Crystalline griseofulvin peaks are present in the diffraction pattern of the griseofulvin-loaded PLGA/PCL particles, most prominently at 16.6° and 26.7°. However, it was not determined whether the

crystals grew within the particles or externally from the bulk solution during formation.

**3.6. Further Discussion.** The compartmental, heterogenic nature of anisotropic colloidal particles presents the opportunity for multiple functionalities within the same particle. Their interesting chemical, optical, and electrical properties set them apart from traditional spherical, isotropic particles. Therefore, the ABMPs and ABNPs shown in this work have countless applications in pharmaceuticals, biomedicine, materials science, and dispersion stabilization. These particles can be tailored to many applications, such as active and passive drug carriers, foams, emulsions, colloidal gels, scaffolds, or even hybrid-Janus materials.<sup>2,17</sup> Anisotropic “Janus” particles have been incorporated in electronic display devices, sensors, and solar cells<sup>18,19</sup> or even employed as substitutions for traditional surfactants.<sup>20,21</sup>

Biodegradable ABMPs offer a platform for sequential compartmentalized dual drug delivery, where release of the active agent from each compartment is intrinsically dependent upon the degradation rate of the encapsulating polymer. Since one compartment is more hydrophobic than the other, it is assumed that the drug with the higher log *P* value will segregate to the more hydrophobic compartment while the less hydrophobic drug will segregate to the less hydrophobic compartment. In the case of hydrophilic or lipophilic drugs, the polymer/lipid particles would be employed and the hydrophilic or lipophilic drug would reside within the lipid phase.

Drug release rate may be more precisely controlled by employing stimuli-responsive polymers that degrade under predetermined conditions, such as change in pH or temperature. The ability to manipulate release profiles of multiple agents is of particular importance in treating specific diseases that require exposure to one active agent at a specific rate, followed by exposure to the next active agent at a different rate. Such staggered release profiles would be beneficial in treating many types of cancers, which develop resistance when the same chemotherapeutic agent is consistently administered over time. Specifically, it has been reported that coadministration of chemotherapy and multiple antiangiogenic agents or suppressor genes that silence the multidrug resistance (MDR) pathway provides the maximal therapeutic benefit when treating cancerous tumors.<sup>22,23</sup> ABMPs are the only self-contained entities capable of providing multicompartmental drug delivery with staggered drug release rates.

Anisotropic particles inherently present different surface areas than spherical isotropic particles, which allows for greater flexibility in the design of targeted nanoparticles. The added surface area is due to the regions of curvature at the interface, thus offering more area for functionalization. Although targeting ligands confer specificity, they also negatively impact particle surface properties. Introducing targeting ligands compromises the PEG surface coating, resulting in faster particle clearance by the RES.<sup>24,25</sup> Nanoparticle surface must be optimized in terms of PEG and targeting ligand coverage to provide for both prolonged circulation times necessary to reach the target and selective cellular binding at the target. The altered surface area offered by anisotropic particles is of particular interest because of the ability to fit enough targeting ligands on the particle surface while retaining sufficient PEG coverage. Furthermore, the presence of two different surfaces ensures that there is adequate space for attachment of multiple targeting ligands. Dual targeting is especially enticing for platforms targeting diseases of the CNS, which must not only

localize to the affected area but also overcome the highly selective blood–brain barrier (BBB). Anisotropic particles can accommodate coattachment of ligands that participate in receptor-mediated transcytosis across the BBB and ligands that target receptors overexpressed on diseased cell membranes.

Precirol-containing particles similar to those formulated in this work are widely used in topical drug delivery.<sup>11</sup> The hybrid polymer/lipid particle formulation provides the advantages of using both lipids and polymers, while avoiding their limitations.<sup>25</sup> Polymer/lipid ABMPs are attractive drug carriers because their polymeric core has a high drug loading efficiency, and the surrounding lipid may serve as a buffer layer to achieve maximal drug retention within the core. The lipid layer prevents drug molecules from diffusing out of the polymeric core and reduces water penetration into the core.<sup>25</sup> This lipid layer also slows degradation of the polymer, providing for even greater in vivo stability and extended drug release. Inclusion of a lipid component also facilitates encapsulation of lipophilic drugs, otherwise a challenge for the hydrophobic PLGA and PCL.

Finally, colloids have an inherent tendency to agglomerate, and surfactants are typically used for stabilization. However, most surfactants are regarded as harmful or even toxic in large quantities. Combining two GRAS polymers to form a small, anisotropic biodegradable particle with amphiphilic surfactant-like properties is a promising alternative to replace surfactants as a hydrosol or Pickering emulsion formulation for pharmaceutical and cosmetic products including emulsions, foams, dispersions, and coatings.

#### 4. CONCLUSIONS

The modified emulsion solvent evaporation method employed was used to produce several formulations of anisotropic biodegradable micro- and nanoparticles (ABMPs and ABNPs). Compartmentalized ABMPs were produced from binary mixtures of the widely used biodegradable polymers PLGA and PCL. Unique “ice cream cone” particles were produced from combining either PLGA or PCL with the biodegradable lipid Precirol. A preliminary investigation of drug loading indicated that addition of drug significantly altered phase segregation of polymer/polymer particle formation and resulted in “pox-like” spherical particles with phase-separated polymer blisters on the surface. Compartmentalization and anisotropy were confirmed for ABMPs through laser diffraction, optical and scanning electron microscopy, zeta potential, X-ray diffraction, and electrophoresis. It is the authors’ hope that the results of this study will pave the way for further studies investigating potential applications of these novel ABMPs and ABNPs.

#### ■ AUTHOR INFORMATION

##### Corresponding Author

\*E-mail: silvina@soemail.rutgers.edu.

##### Notes

The authors declare no competing financial interest.

#### ■ ACKNOWLEDGMENTS

We would like to acknowledge the support of the NSF-IGERT for NanoPharmaceutical Engineering and Science, grant no. 0504497, and NSF ERC-SOPS center, grant EEC-0540855. In addition, we thank Dr. Thomas J. Emge and Mr. Valentin Starovoytov from Rutgers University for their assistance.

## ■ REFERENCES

- (1) Lee, K.J.; Yoon, J.; Lahann, J. *Curr. Opin. Colloid Interface Sci.*, in press.
- (2) Chen, Q.; Whitmer, J. K.; Jiang, S.; Bae, S. C.; Luijten, E.; Granick, S. *Science* **2011**, *331*, 199–202.
- (3) Ruzicka, B.; Zaccarelli, E.; Zulian, L.; Angelini, R.; Sztucki, M.; Moussaïd, A.; Narayanan, T.; Sciortino, F. *Nat. Mater.* **2011**, *10*, 56–60.
- (4) Saito, N.; Kagari, Y.; Okubo, M. *Langmuir* **2006**, *22*, 9397–9402.
- (5) Saito, N.; Nakatsuru, R.; Kagari, Y.; Okubo, M. *Langmuir* **2007**, *23*, 11506–11512.
- (6) Shah, R. K.; Kim, J.-W.; Weitz, D. A. *Adv. Mater.* **2009**, *21*, 1949–1953.
- (7) Abate, A. R.; Kutsovsky, M.; Seiffert, S.; Windbergs, M.; Pinto, L. F. V.; Rotem, A.; Utada, A. S.; Weitz, D. A. *Adv. Mater.* **2011**, *23*, 1757–1760.
- (8) He, J.; Hourwitz, M. J.; Liu, Y.; Perez, M. T.; Nie, Z. *Chem. Commun.* **2011**, *47*, 12450–12452.
- (9) Woodruff, M. A.; Hutmacher, D. W. *Prog. Polym. Sci.* **2010**, *35*, 1217–1256.
- (10) Mundargi, R. C.; Babu, V. R.; Rangaswamy, V.; Patel, P.; Aminabhavi, T. M. *J. Controlled Release* **2008**, *125*, 193–209.
- (11) Müller, R. H.; Mäder, K.; Gohla, S. *Eur. J. Pharm. Biopharm.* **2000**, *50*, 161–177.
- (12) Merisko-Liversidge, E.; Liversidge, G. G.; Cooper, E. R. *Eur. J. Pharm. Sci.* **2003**, *18*, 113–120.
- (13) Baker, S. C.; Rohman, G.; Southgate, J.; Cameron, N. R. *Biomaterials* **2009**, *30*, 1321–1328.
- (14) Knox, C.; Law, V.; Jewison, T.; Liu, P.; Ly, S.; Frolkis, A.; Pon, A.; Banco, K.; Mak, C.; Neveu, V.; Djoumbou, Y.; Eisner, R.; Guo, A. C.; Wishart, D. S. *Nucleic Acids Res.* **2011**, *39*, D1035–1041.
- (15) Higuchi, T.; Tajima, A.; Yabu, H.; Shimomura, M. *Soft Matter* **2008**, *4*, 1302–1305.
- (16) Yamamura, S.; Takahira, R.; Momose, Y. *Pharm. Res.* **2007**, *24*, 880–887.
- (17) Furlan, M.; Kluge, J.; Mazzotti, M.; Lattuada, M. *J. Supercrit. Fluids* **2010**, *54*, 348–356.
- (18) Casagrande, C.; et al. *EPL (Europhys. Lett.)* **1989**, *9*, 251.
- (19) Kretzschmar, I.; Song, J. H. *Curr. Opin. Colloid Interface Sci.*, in press.
- (20) Binks, B. P. *Curr. Opin. Colloid Interface Sci.* **2002**, *7*, 21–41.
- (21) Horozov, T. S. *Curr. Opin. Colloid Interface Sci.* **2008**, *13*, 134–140.
- (22) Taberner, J. *Mol. Cancer Res.* **2007**, *5*, 203–220.
- (23) Yadav, S.; van Vlerken, L.; Little, S.; Amiji, M. *Cancer Chemother. Pharmacol.* **2009**, *63*, 711–722.
- (24) Wang, M.; Thanou, M. *Pharmacol. Res.* **2010**, *62*, 90–99.
- (25) Zhang, L.; Zhang, L. *Nano LIFE* **2010**, *1*, 163–173.